

Electronic Supplementary Information

SILAR Deposition of Bismuth Vanadate Photoanodes for Photoelectrochemical Water Splitting

Samantha Prabath Ratnayake¹, Jiawen Ren¹, Joel van Embden¹, Chris F.

*McConville^{1,2}, Enrico Della Gaspera^{1, *}*

¹ School of Science, RMIT University, Melbourne VIC 3000, Australia

² Institute for Frontier Materials, Deakin University, Geelong, VIC 3216, Australia

Corresponding author: *enrico.dellagaspera@rmit.edu.au; jiawen.ren@rmit.edu.au

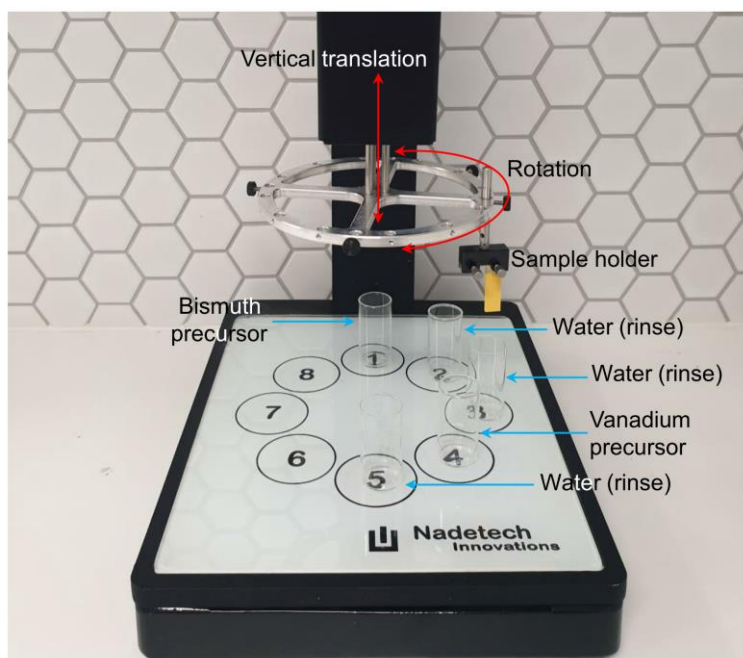


Figure S1. Photograph of the rotary dip coater used for the SILAR deposition highlighting its key components.

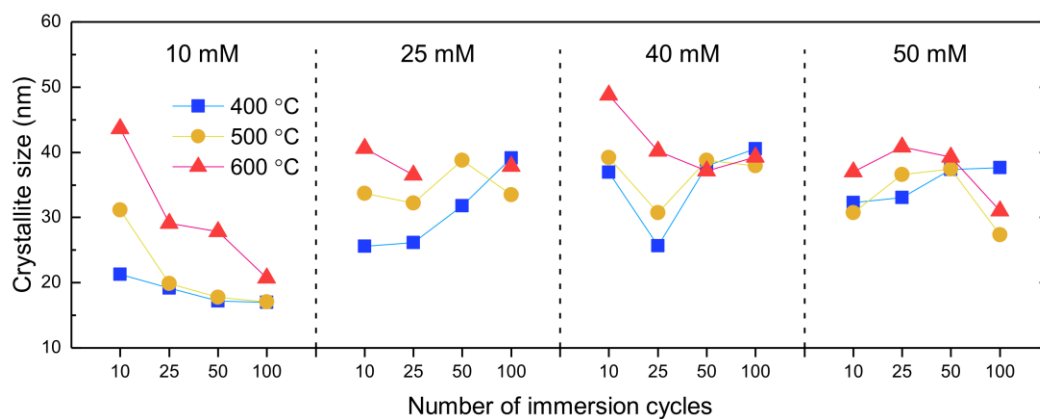


Figure S2. Crystallite size estimated from XRD data using the Scherrer formula applied to the most intense BiVO_4 peak (at $2\theta \sim 29^\circ$) for all the samples prepared in this study as a function of the concentration of the precursor solutions, the number of SILAR cycles and the annealing temperature. Very thin samples (low precursor concentrations and low number of cycles) are omitted due to the very low intensity of the XRD peaks.

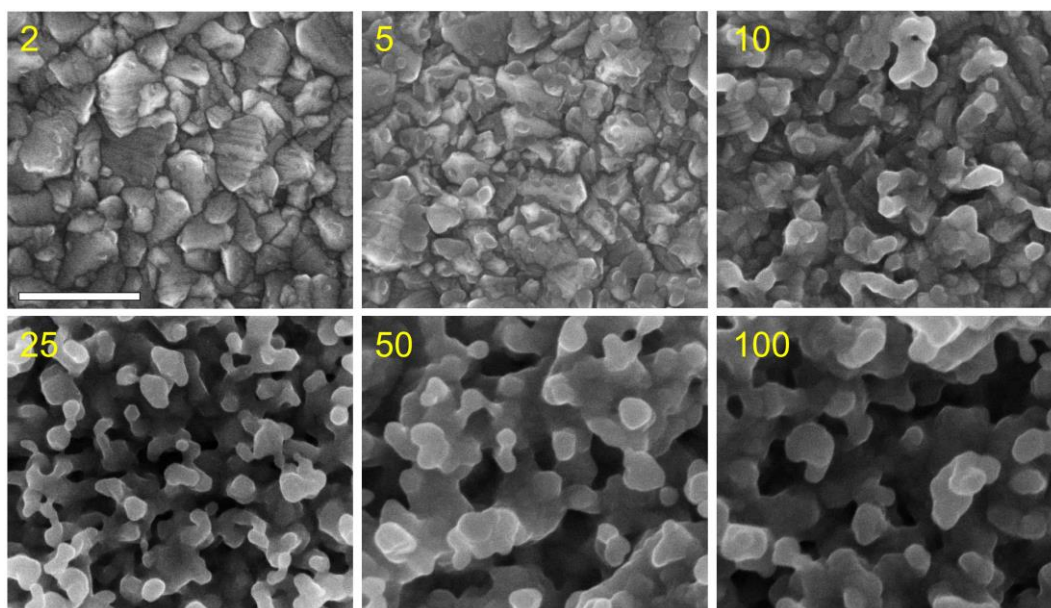


Figure S3. SEM images of BiVO_4 films deposited from 10 mM precursor solutions and annealed at 500 °C as a function of the number of SILAR cycles (from 2 to 100). The scale bar is 500 nm and is common to all images.

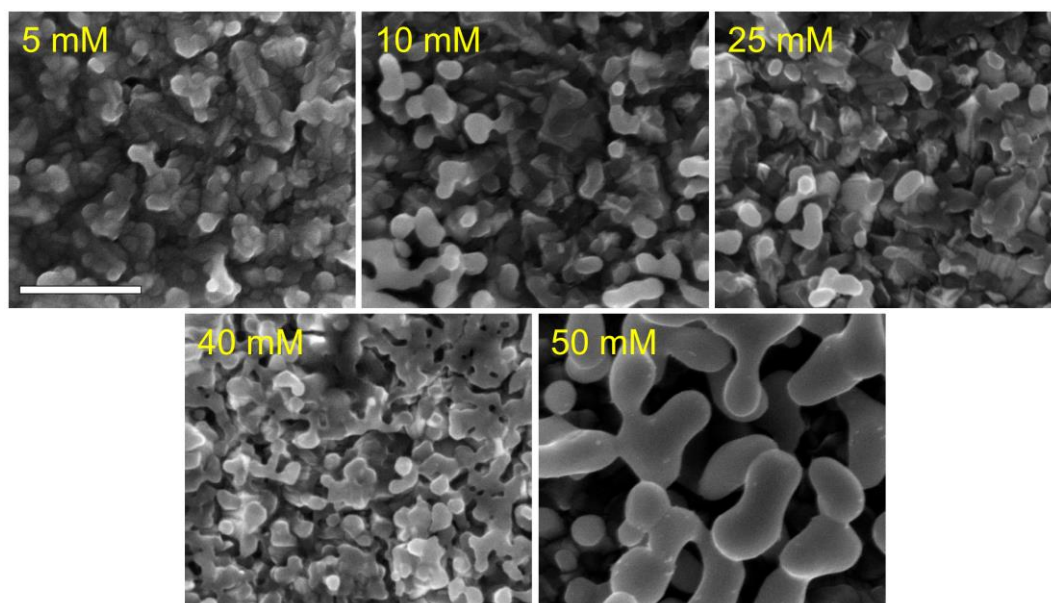


Figure S4. SEM images of BiVO_4 films deposited with 10 SILAR cycles and annealed at 500 °C as a function of the concentration of the precursor solutions (from 5 mM to 50 mM). The scale bar is 500 nm and is common to all images.

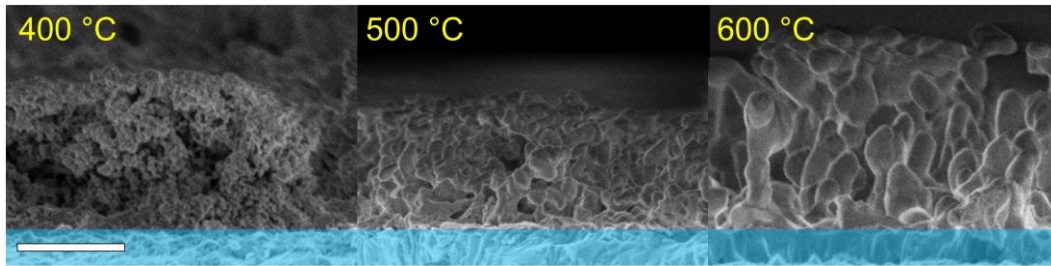


Figure S5. SEM images in cross section for BiVO_4 films annealed at different temperatures. The FTO substrate is highlighted in blue. The scale bar is $1\ \mu\text{m}$ and is common to all images.

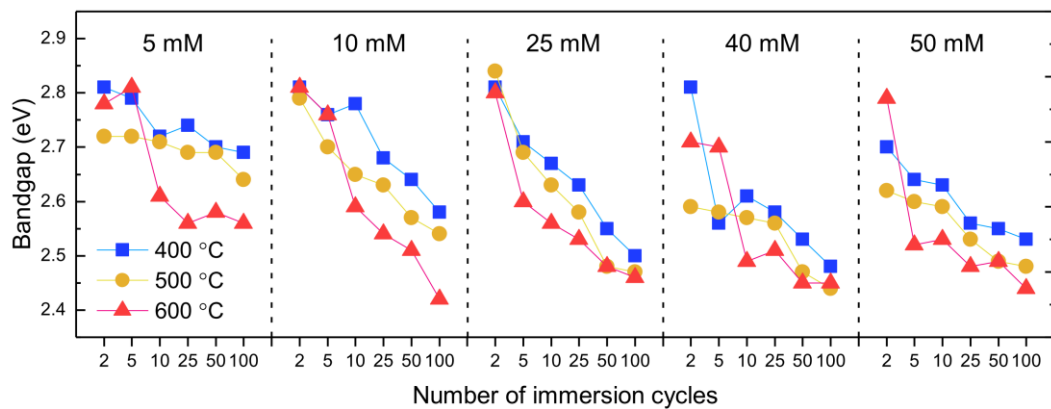


Figure S6. Band gap estimation for all the samples prepared in this study as a function of the concentration of the precursor solutions, the number of SILAR cycles and the annealing temperature.

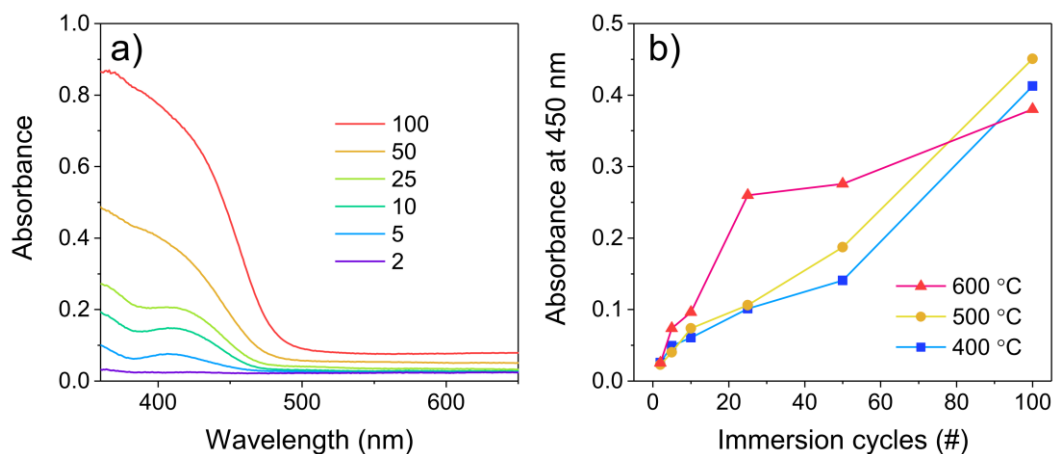


Figure S7. a) Absorbance spectra of BiVO_4 films with varying SILAR cycles (5 mM precursor concentration, $500\ ^\circ\text{C}$ annealing temperature). b) Absorbance measured at 450 nm for BiVO_4 samples deposited with increasing deposition cycles and annealed at different temperatures. A progressive increase in absorption with the number of SILAR cycles is observed at all annealing temperatures.

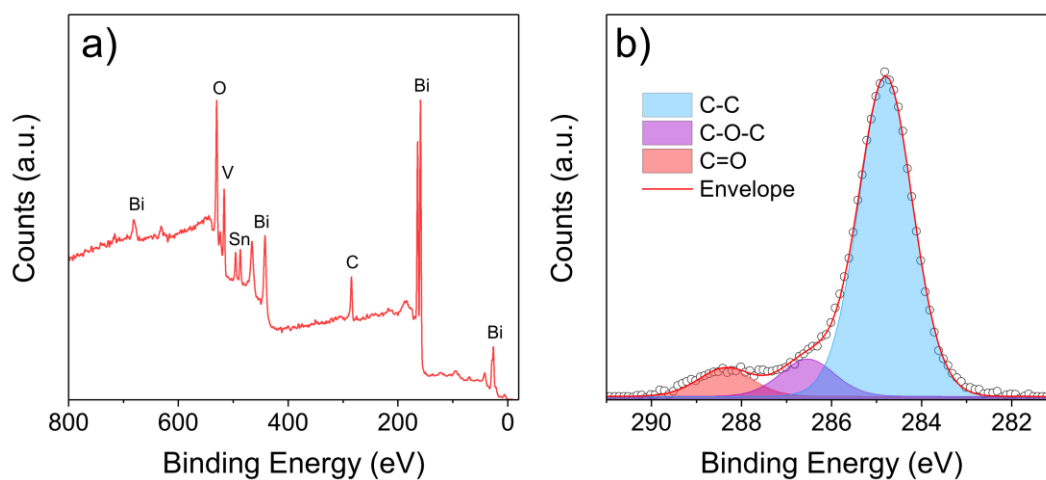


Figure S8. a) XPS survey spectrum of a BiVO_4 film annealed at 600 °C. b) XPS spectrum in the C 1s region and related peak fittings.

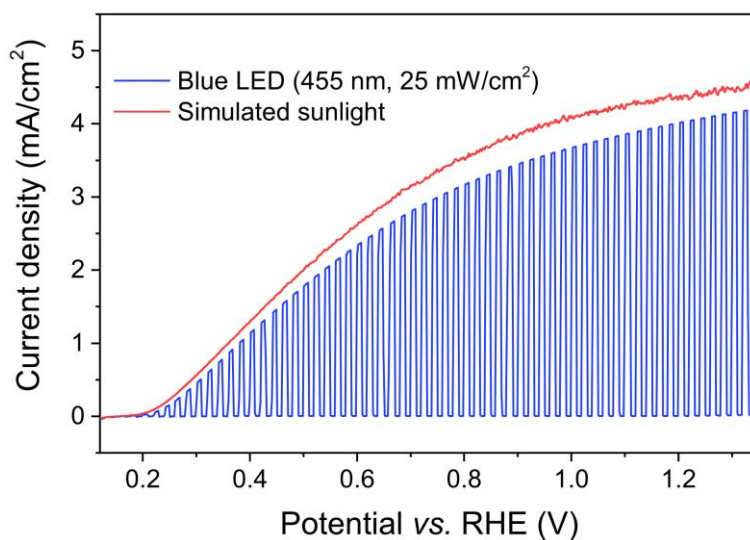


Figure S9. Current-Voltage scan for one of the best BiVO_4 photoanodes in borate buffer with sulfite hole scavenger under blue LED chopped irradiation (25 mW/cm²) and under simulated sunlight (100 mW/cm², AM 1.5 G).

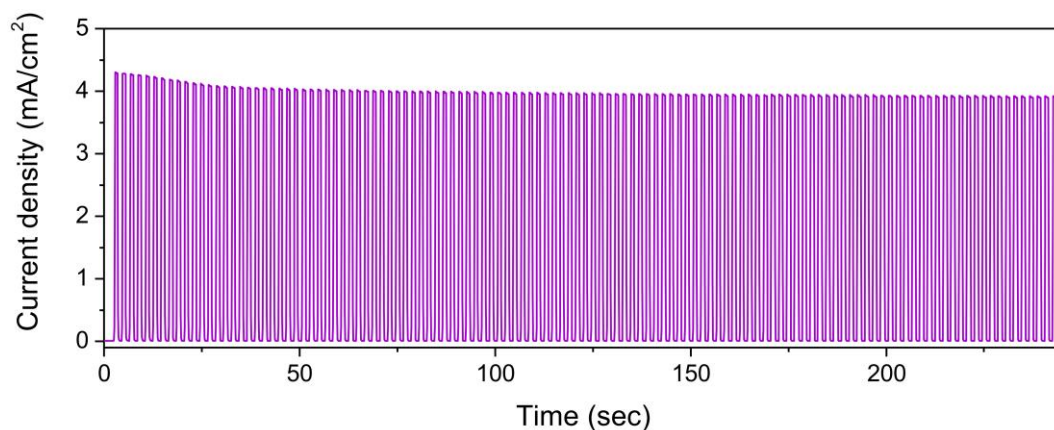


Figure S10. Chronoamperometry under blue LED chopped irradiation at 1.23 V vs. RHE for one of the best BiVO₄ photoanodes in the presence of sulfite buffer. This is the same data presented in Figure 5b, but shown without axes breaks.

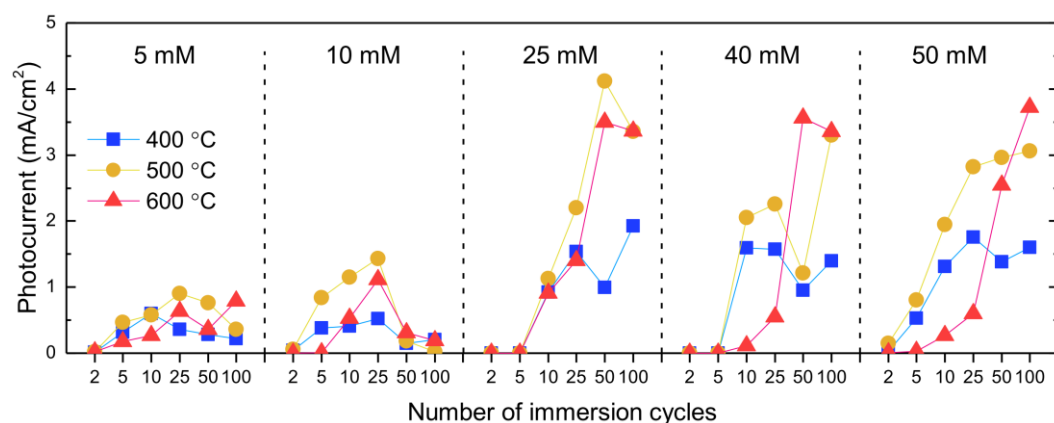


Figure S11. Photocurrent density measured at 1.23 V vs. RHE in sulfite buffer under blue LED irradiation for all the samples prepared in this study as a function of the concentration of the precursor solutions, the number of SILAR cycles and the annealing temperature.

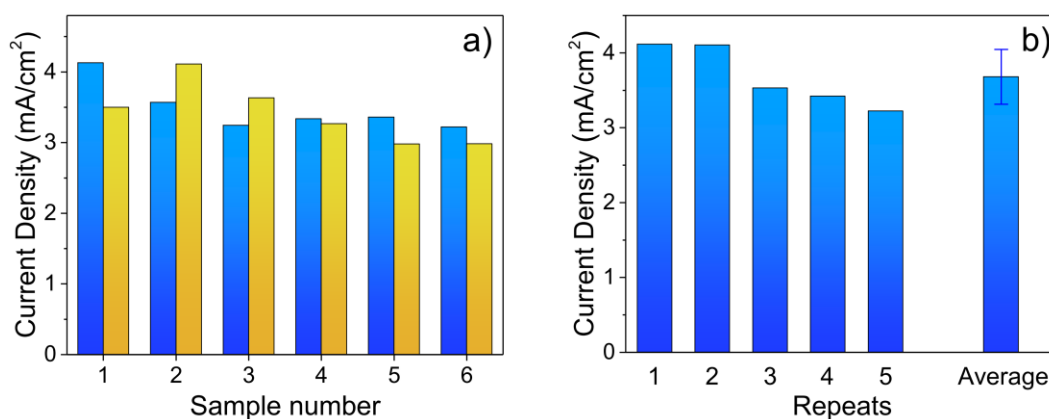


Figure S12. Photocurrent density measured at 1.23 V vs. RHE in sulfite buffer under blue LED irradiation for a) six samples prepared in different conditions producing a photocurrent greater than 3 mA/cm² and their repeats; b) five repeats of the same sample conditions, including average and standard deviation. The order of the samples and the repeats (with decreasing photocurrent from left to right) has been chosen on purpose and does not represent a chronological order.

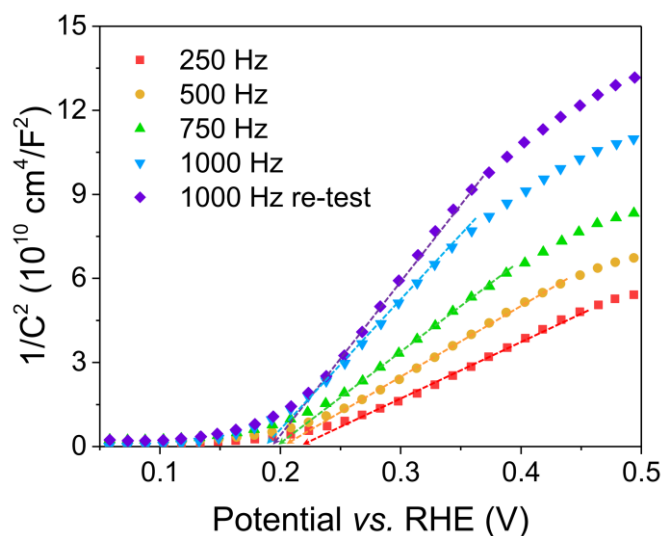


Figure S13. Mott-Schottky plot for a BiVO₄ sample after FeOOH/NiOOH deposition conducted at different frequencies. The flat band potential is seen to vary only between 0.19 V and 0.22 V, suggesting good reproducibility of the results.

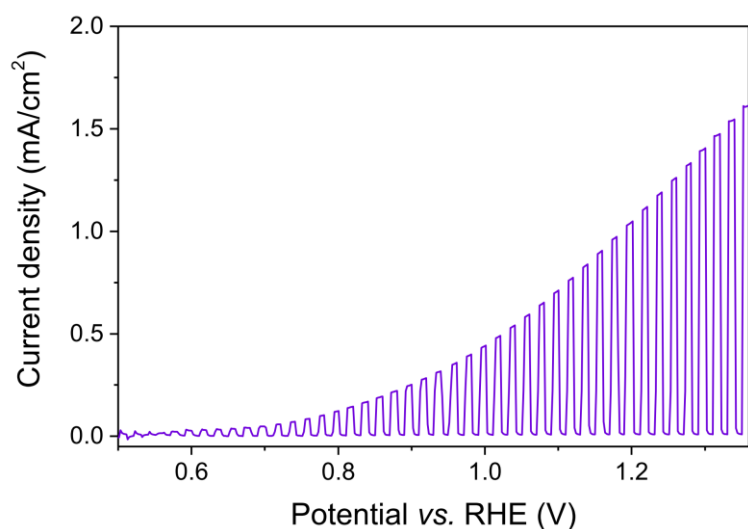


Figure S14. Current-Voltage scan for one of the best BiVO₄ photoanodes in pure borate buffer (without sulfite) under blue LED chopped irradiation.

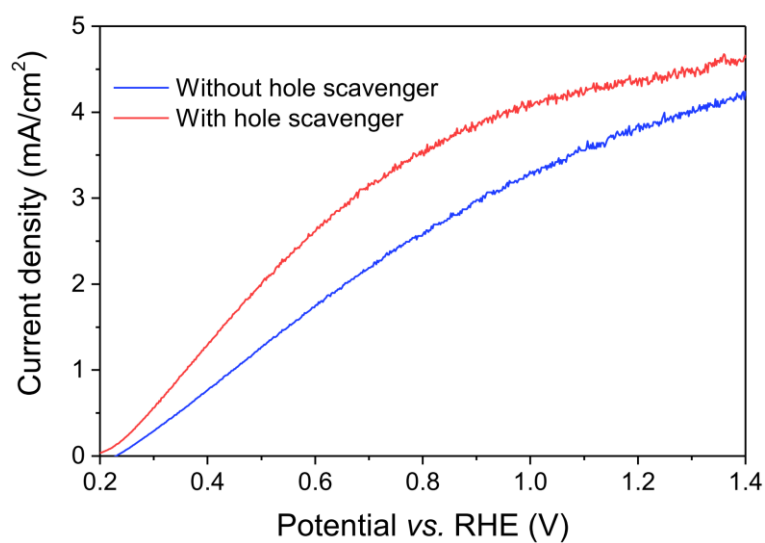


Figure S15. Current-Voltage scan for one of the best BiVO₄ photoanodes after deposition of the NiOOH/FeOOH OER catalysts in borate buffer with and without sulfite under simulated sunlight irradiation.

Discussion on Mott-Schottky analysis

Depending on the carrier donor density (N_d) of the film, the M-S equation can be defined with two different relationships. When $N_d < 10^{20} \text{ cm}^{-3}$, a Boltzmann distribution of carriers is assumed, and the M-S equation is:

$$\frac{1}{C^2} = \left(\frac{2}{e\epsilon\epsilon_0 N_d A^2} \right) \left(V_a - V_{fb} - \frac{k_B T}{e} \right)$$

where C is the space charge layers capacitance, e is the electron charge, ϵ is the dielectric constant ($\epsilon = 68$ for BiVO_4)¹, ϵ_0 is the permittivity of vacuum, A is the exposed area of the sample to the electrolyte, V_a is the applied potential, V_{fb} is the flat-band potential, k_B is the Boltzmann constant, and T is the absolute temperature.²

If $N_d > 10^{20} \text{ cm}^{-3}$, more general Fermi-Dirac statistics need to be applied, and the M-S equation becomes:

$$\frac{1}{C^2} = \left(\frac{2}{e\epsilon\epsilon_0 N_d A^2} \right) \left(V_a - V_{fb} - \frac{2 E_f}{5 e} \right)$$

where

$$E_f = \frac{[\hbar^2 (3\pi^2 N_d)^{2/3}]}{2m^*}$$

is the Fermi level energy, and m^* is the effective electron mass (for BiVO_4 , $m^*=0.55m_e$).²

Supporting references

1. Ma, Y.; Pendlebury, S. R.; Reynal, A.; Le Formal, F.; Durrant, J. R., Dynamics of photogenerated holes in undoped BiVO_4 photoanodes for solar water oxidation. *Chemical Science* **2014**, 5 (8), 2964-2973.
2. Nasir, S. N. S.; Mohamed, N. A.; Tukimon, M. A.; Noh, M. F. M.; Arzaee, N. A.; Teridi, M. A. M., Direct extrapolation techniques on the energy band diagram of BiVO_4 thin films. *Physica B: Condensed Matter* **2021**, 604, 412719.